Search for ZZ and $Z\gamma^*$ production in $p\bar{p}$ collisions at $\sqrt{s}$ = 1.96 TeV and limits on anomalous ZZZ and $ZZ\gamma^*$ couplings

V.M. Abazov, B. Abbott, M. Abolins, B.S. Acharya, M. Adams, T. Adams, E. Aguil, S.H. Ahn, M. Ahsan, G.D. Alexeev, et al.

FERMILAB-PUB-07-641-E

Search for ZZ and $Z\gamma^*$ production in $p\bar{p}$ collisions at $\sqrt{s} = 1.96$ TeV and limits on anomalous ZZZ and $ZZ\gamma^*$ couplings

V.M. Abazov[36], B. Abbott[76], M. Abolins[66], B.S. Acharya[29], M. Adams[52], T. Adams[50], E. Aguilo[6], S.H. Ahn[31], M. Ahsan[60], G.D. Alexeev[36], G. Alkhazov[40], A. Alton[65,a], G. Alverson[64], G.A. Alves[2], M. Anastasoaie[35], L.S. Ancu[35], T. Andeen[54], S. Anderson[46], B. Andrieu[17], M.S. Anzelc[54], Y. Arnoud[14], M. Arov[61], M. Arthaud[18], A. Askew[50], B. Åsman[41], A.C.S. Assis Jesus[3], O. Atramentov[50], C. Autermann[21], C. Avila[8], C. Ay[24], F. Badaud[13], A. Baden[62], L. Bagby[53], B. Baldin[51], D.V. Bandurin[60], S. Banerjee[29], P. Banerjee[29], E. Barberis[64], A.-F. Barfuss[15], P. Bargassa[81], P. Baringer[59], J. Barreto[2], J.F. Bartlett[51], U. Bassler[18], D. Bauer[44], S. Beale[6], A. Bean[59], M. Begalli[3], M. Begel[72], C. Belanger-Champagne[41], L. Bellantoni[51], A. Bellavance[51], J.A. Benitez[66], S.B. Beri[27], G. Bernardi[17], R. Bernhard[23], I. Bertram[43], M. Besançon[18], R. Beuselinck[44], V.A. Bezzubov[39], P.C. Bhat[51], V. Bhatnagar[27], C. Biscarat[20], G. Blazey[53], F. Blekman[44], S. Blessing[50], D. Bloch[19], K. Bloom[68], A. Boehnlein[51], D. Boline[63], T.A. Bolton[60], G. Borissov[43], T. Bose[78], A. Brandt[79], R. Brock[66], G. Brooijmans[71], A. Bross[51], D. Brown[82], N.J. Buchanan[50], D. Buchholz[54], M. Buehler[82], V. Buescher[22], V. Bunichev[38], S. Burdin[43,b], S. Burke[46], T.H. Burnett[83], C.P. Buszello[44], J.M. Butler[63], P. Calfayan[25], S. Calvet[16], J. Cammin[72], W. Carvalho[3], B.C.K. Casey[51], N.M. Cason[56], H. Castilla-Valdez[33], S. Chakrabarti[18], D. Chakraborty[53], K.M. Chan[56], K. Chan[6], A. Chandra[49], F. Charles[19,‡], E. Cheu[46], F. Chevallier[14], D.K. Cho[63], S. Choi[32], B. Choudhary[28], L. Christofek[78], T. Christoudias[44,†], S. Cihangir[51], D. Claes[68], Y. Coadou[6], M. Cooke[81], W.E. Cooper[51], M. Corcoran[81], F. Couderc[18], M.-C. Cousinou[15], S. Crépé-Renaudin[14], D. Cutts[78], M. Ćwiok[30], H. da Motta[2], A. Das[46], G. Davies[44], K. De[79], S.J. de Jong[35], E. De La Cruz-Burelo[65], C. De Oliveira Martins[3], J.D. Degenhardt[65], F. Déliot[18], M. Demarteau[51], R. Demina[72], D. Denisov[51], S.P. Denisov[39], S. Desai[51], H.T. Diehl[51], M. Diesburg[51], A. Dominguez[68], H. Dong[73], L.V. Dudko[38], L. Duflot[16], S.R. Dugad[29], D. Duggan[50], A. Duperrin[15], J. Dyer[66], A. Dyshkant[53], M. Eads[68], D. Edmunds[66], J. Ellison[49], V.D. Elvira[51], Y. Enari[78], S. Eno[62], P. Ermolov[38], H. Evans[55], A. Evdokimov[74], V.N. Evdokimov[39], A.V. Ferapontov[60], T. Ferbel[72], F. Fiedler[24], F. Filthaut[35], W. Fisher[51], H.E. Fisk[51], M. Ford[45], M. Fortner[53], H. Fox[23], S. Fu[51], S. Fuess[51], T. Gadfort[83], C.F. Galea[35], E. Gallas[51], E. Galyaev[56], C. Garcia[72], A. Garcia-Bellido[83], V. Gavrilov[37], P. Gay[13], W. Geist[19], D. Gelé[19], C.E. Gerber[52], Y. Gershtein[50], D. Gillberg[6], G. Ginther[72], N. Gollub[41], B. Gómez[8], A. Goussiou[56], P.D. Grannis[73], H. Greenlee[51], Z.D. Greenwood[61], E.M. Gregores[4], G. Grenier[20], Ph. Gris[13], J.-F. Grivaz[16], A. Grohsjean[25], S. Grünendahl[51], M.W. Grünewald[30], J. Guo[73], F. Guo[73], P. Gutierrez[76], G. Gutierrez[51], A. Haas[71], N.J. Hadley[62], P. Haefner[25], S. Hagopian[50], J. Haley[69], I. Hall[66], R.E. Hall[48], L. Han[7], K. Hanagaki[51], P. Hansson[41], K. Harder[45], A. Harel[72], R. Harrington[64], J.M. Hauptman[58], R. Hauser[66], J. Hays[44], T. Hebbeker[21], D. Hedin[53], J.G. Hegeman[34], J.M. Heinmiller[52], A.P. Heinson[49], U. Heintz[63], C. Hensel[59], K. Herner[73], G. Hesketh[64], M.D. Hildreth[56], R. Hirosky[82], J.D. Hobbs[73], B. Hoeneisen[12], H. Hoeth[26], M. Hohlfeld[22], S.J. Hong[31], S. Hossain[76], P. Houben[34], Y. Hu[73], Z. Hubacek[10], V. Hynek[9], I. Iashvili[70], R. Illingworth[51], A.S. Ito[51], S. Jabeen[63], M. Jaffré[16], S. Jain[76], K. Jakobs[23], C. Jarvis[62], R. Jesik[44], K. Johns[46], C. Johnson[71], M. Johnson[51], A. Jonckheere[51], P. Jonsson[44], A. Juste[51], D. Käfer[21], E. Kajfasz[15], A.M. Kalinin[36], J.R. Kalk[66], J.M. Kalk[61], S. Kappler[21], D. Karmanov[38], P. Kasper[51], I. Katsanos[71], D. Kau[50], R. Kaur[27], V. Kaushik[79], R. Kehoe[80], S. Kermiche[15], N. Khalatyan[51], A. Khanov[77], A. Kharchilava[70], Y.M. Kharzheev[36], D. Khatidze[71], H. Kim[32], T.J. Kim[31], M.H. Kirby[54], M. Kirsch[21], B. Klima[51], J.M. Kohli[27], J.-P. Konrath[23], M. Kopal[76], V.M. Korablev[39], A.V. Kozelov[39], D. Krop[55], T. Kuhl[24], A. Kumar[70], S. Kunori[62], A. Kupco[11], T. Kurča[20], J. Kvita[9], F. Lacroix[13], D. Lam[56], S. Lammers[71], G. Landsberg[78], P. Lebrun[20], W.M. Lee[51], A. Leflat[38], F. Lehner[42], J. Lellouch[17], J. Leveque[46], P. Lewis[44], J. Li[79], Q.Z. Li[51], L. Li[49], S.M. Lietti[5], J.G.R. Lima[53], D. Lincoln[51], J. Linnemann[66], V.V. Lipaev[39], R. Lipton[51], Y. Liu[7,†], Z. Liu[6], L. Lobo[44], A. Lobodenko[40], M. Lokajicek[11], P. Love[43], H.J. Lubatti[83], A.L. Lyon[51], A.K.A. Maciel[2], D. Mackin[81], R.J. Madaras[47], P. Mättig[26], C. Magass[21], A. Magerkurth[65], P.K. Mal[56], H.B. Malbouisson[3], S. Malik[68], V.L. Malyshev[36], H.S. Mao[51], Y. Maravin[60], B. Martin[14], R. McCarthy[73], A. Melnitchouk[67], A. Mendes[15], L. Mendoza[8], P.G. Mercadante[5], M. Merkin[38], K.W. Merritt[51], J. Meyer[22,d], A. Meyer[21], T. Millet[20], J. Mitrevski[71], J. Molina[3], R.K. Mommsen[45], N.K. Mondal[29], R.W. Moore[6], T. Moulik[59], G.S. Muanza[20], M. Mulders[51], M. Mulhearn[71], O. Mundal[22], L. Mundim[3], E. Nagy[15], M. Naimuddin[51], M. Narain[78], N.A. Naumann[35], H.A. Neal[65], J.P. Negret[8], P. Neustroev[40], H. Nilsen[23], H. Nogima[3], A. Nomerotski[51], S.F. Novaes[5], T. Nunnemann[25], V. O'Dell[51], D.C. O'Neil[6], G. Obrant[40], C. Ochando[16], D. Onoprienko[60],

N. Oshima[51], J. Osta[56], R. Otec[10], G.J. Otero y Garzón[51], M. Owen[45], P. Padley[81], M. Pangilinan[78], N. Parashar[57], S.-J. Park[72], S.K. Park[31], J. Parsons[71], R. Partridge[78], N. Parua[55], A. Patwa[74], G. Pawloski[81], B. Penning[23], M. Perfilov[38], K. Peters[45], Y. Peters[26], P. Pétroff[16], M. Petteni[44], R. Piegaia[1], J. Piper[66], M.-A. Pleier[22], P.L.M. Podesta-Lerma[33,c], V.M. Podstavkov[51], Y. Pogorelov[56], M.-E. Pol[2], P. Polozov[37], B.G. Pope[66], A.V. Popov[39], C. Potter[6], W.L. Prado da Silva[3], H.B. Prosper[50], S. Protopopescu[74], J. Qian[65], A. Quadt[22,d], B. Quinn[67], A. Rakitine[43], M.S. Rangel[2], K. Ranjan[28], P.N. Ratoff[43], P. Renkel[80], S. Reucroft[64], P. Rich[45], M. Rijssenbeek[73], I. Ripp-Baudot[19], F. Rizatdinova[77], S. Robinson[44], R.F. Rodrigues[3], M. Rominsky[76], C. Royon[18], P. Rubinov[51], R. Ruchti[56], G. Safronov[37], G. Sajot[14], A. Sánchez-Hernández[33], M.P. Sanders[17], A. Santoro[3], G. Savage[51], L. Sawyer[61], T. Scanlon[44], D. Schaile[25], R.D. Schamberger[73], Y. Scheglov[40], H. Schellman[54], P. Schieferdecker[25], T. Schliephake[26], C. Schwanenberger[45], A. Schwartzman[69], R. Schwienhorst[66], J. Sekaric[50], H. Severini[76], E. Shabalina[52], M. Shamim[60], V. Shary[18], A.A. Shchukin[39], R.K. Shivpuri[28], V. Siccardi[19], V. Simak[10], V. Sirotenko[51], P. Skubic[76], P. Slattery[72], D. Smirnov[56], J. Snow[75], G.R. Snow[68], S. Snyder[74], S. Söldner-Rembold[45], L. Sonnenschein[17], A. Sopczak[43], M. Sosebee[79], K. Soustruznik[9], M. Souza[2], B. Spurlock[79], J. Stark[14], J. Steele[61], V. Stolin[37], D.A. Stoyanova[39], J. Strandberg[65], S. Strandberg[41], M.A. Strang[70], M. Strauss[76], E. Strauss[73], R. Ströhmer[25], D. Strom[54], L. Stutte[51], S. Sumowidagdo[50], P. Svoisky[56], A. Sznajder[3], M. Talby[15], P. Tamburello[46], A. Tanasijczuk[1], W. Taylor[6], J. Temple[46], B. Tiller[25], F. Tissandier[13], M. Titov[18], V.V. Tokmenin[36], T. Toole[62], I. Torchiani[23], T. Trefzger[24], D. Tsybychev[73], B. Tuchming[18], C. Tully[69], P.M. Tuts[71], R. Unalan[66], S. Uvarov[40], L. Uvarov[40], S. Uzunyan[53], B. Vachon[6], P.J. van den Berg[34], R. Van Kooten[55], W.M. van Leeuwen[34], N. Varelas[52], E.W. Varnes[46], I.A. Vasilyev[39], M. Vaupel[26], P. Verdier[20], L.S. Vertogradov[36], M. Verzocchi[51], F. Villeneuve-Seguier[44], P. Vint[44], P. Vokac[10], E. Von Toerne[60], M. Voutilainen[68,e], R. Wagner[69], H.D. Wahl[50], L. Wang[62], M.H.L.S Wang[51], J. Warchol[56], G. Watts[83], M. Wayne[56], M. Weber[51], G. Weber[24], A. Wenger[23,f], N. Wermes[22], M. Wetstein[62], A. White[79], D. Wicke[26], G.W. Wilson[59], S.J. Wimpenny[49], M. Wobisch[61], D.R. Wood[64], T.R. Wyatt[45], Y. Xie[78], S. Yacoob[54], R. Yamada[51], M. Yan[62], T. Yasuda[51], Y.A. Yatsunenko[36], K. Yip[74], H.D. Yoo[78], S.W. Youn[54], J. Yu[79], A. Zatserklyaniy[53], C. Zeitnitz[26], T. Zhao[83], B. Zhou[65], J. Zhu[73], M. Zielinski[72], D. Zieminska[55], A. Zieminski[55,‡], L. Zivkovic[71], V. Zutshi[53], and E.G. Zverev[38]

(The DØ Collaboration)

[1] *Universidad de Buenos Aires, Buenos Aires, Argentina*
[2] *LAFEX, Centro Brasileiro de Pesquisas Físicas, Rio de Janeiro, Brazil*
[3] *Universidade do Estado do Rio de Janeiro, Rio de Janeiro, Brazil*
[4] *Universidade Federal do ABC, Santo André, Brazil*
[5] *Instituto de Física Teórica, Universidade Estadual Paulista, São Paulo, Brazil*
[6] *University of Alberta, Edmonton, Alberta, Canada, Simon Fraser University, Burnaby, British Columbia, Canada, York University, Toronto, Ontario, Canada, and McGill University, Montreal, Quebec, Canada*
[7] *University of Science and Technology of China, Hefei, People's Republic of China*
[8] *Universidad de los Andes, Bogotá, Colombia*
[9] *Center for Particle Physics, Charles University, Prague, Czech Republic*
[10] *Czech Technical University, Prague, Czech Republic*
[11] *Center for Particle Physics, Institute of Physics, Academy of Sciences of the Czech Republic, Prague, Czech Republic*
[12] *Universidad San Francisco de Quito, Quito, Ecuador*
[13] *Laboratoire de Physique Corpusculaire, IN2P3-CNRS, Université Blaise Pascal, Clermont-Ferrand, France*
[14] *Laboratoire de Physique Subatomique et de Cosmologie, IN2P3-CNRS, Universite de Grenoble 1, Grenoble, France*
[15] *CPPM, IN2P3-CNRS, Université de la Méditerranée, Marseille, France*
[16] *Laboratoire de l'Accélérateur Linéaire, IN2P3-CNRS et Université Paris-Sud, Orsay, France*
[17] *LPNHE, IN2P3-CNRS, Universités Paris VI and VII, Paris, France*
[18] *DAPNIA/Service de Physique des Particules, CEA, Saclay, France*
[19] *IPHC, Université Louis Pasteur et Université de Haute Alsace, CNRS, IN2P3, Strasbourg, France*
[20] *IPNL, Université Lyon 1, CNRS/IN2P3, Villeurbanne, France and Université de Lyon, Lyon, France*
[21] *III. Physikalisches Institut A, RWTH Aachen, Aachen, Germany*
[22] *Physikalisches Institut, Universität Bonn, Bonn, Germany*
[23] *Physikalisches Institut, Universität Freiburg, Freiburg, Germany*
[24] *Institut für Physik, Universität Mainz, Mainz, Germany*

[25] Ludwig-Maximilians-Universität München, München, Germany
[26] Fachbereich Physik, University of Wuppertal, Wuppertal, Germany
[27] Panjab University, Chandigarh, India
[28] Delhi University, Delhi, India
[29] Tata Institute of Fundamental Research, Mumbai, India
[30] University College Dublin, Dublin, Ireland
[31] Korea Detector Laboratory, Korea University, Seoul, Korea
[32] SungKyunKwan University, Suwon, Korea
[33] CINVESTAV, Mexico City, Mexico
[34] FOM-Institute NIKHEF and University of Amsterdam/NIKHEF, Amsterdam, The Netherlands
[35] Radboud University Nijmegen/NIKHEF, Nijmegen, The Netherlands
[36] Joint Institute for Nuclear Research, Dubna, Russia
[37] Institute for Theoretical and Experimental Physics, Moscow, Russia
[38] Moscow State University, Moscow, Russia
[39] Institute for High Energy Physics, Protvino, Russia
[40] Petersburg Nuclear Physics Institute, St. Petersburg, Russia
[41] Lund University, Lund, Sweden, Royal Institute of Technology and Stockholm University, Stockholm, Sweden, and Uppsala University, Uppsala, Sweden
[42] Physik Institut der Universität Zürich, Zürich, Switzerland
[43] Lancaster University, Lancaster, United Kingdom
[44] Imperial College, London, United Kingdom
[45] University of Manchester, Manchester, United Kingdom
[46] University of Arizona, Tucson, Arizona 85721, USA
[47] Lawrence Berkeley National Laboratory and University of California, Berkeley, California 94720, USA
[48] California State University, Fresno, California 93740, USA
[49] University of California, Riverside, California 92521, USA
[50] Florida State University, Tallahassee, Florida 32306, USA
[51] Fermi National Accelerator Laboratory, Batavia, Illinois 60510, USA
[52] University of Illinois at Chicago, Chicago, Illinois 60607, USA
[53] Northern Illinois University, DeKalb, Illinois 60115, USA
[54] Northwestern University, Evanston, Illinois 60208, USA
[55] Indiana University, Bloomington, Indiana 47405, USA
[56] University of Notre Dame, Notre Dame, Indiana 46556, USA
[57] Purdue University Calumet, Hammond, Indiana 46323, USA
[58] Iowa State University, Ames, Iowa 50011, USA
[59] University of Kansas, Lawrence, Kansas 66045, USA
[60] Kansas State University, Manhattan, Kansas 66506, USA
[61] Louisiana Tech University, Ruston, Louisiana 71272, USA
[62] University of Maryland, College Park, Maryland 20742, USA
[63] Boston University, Boston, Massachusetts 02215, USA
[64] Northeastern University, Boston, Massachusetts 02115, USA
[65] University of Michigan, Ann Arbor, Michigan 48109, USA
[66] Michigan State University, East Lansing, Michigan 48824, USA
[67] University of Mississippi, University, Mississippi 38677, USA
[68] University of Nebraska, Lincoln, Nebraska 68588, USA
[69] Princeton University, Princeton, New Jersey 08544, USA
[70] State University of New York, Buffalo, New York 14260, USA
[71] Columbia University, New York, New York 10027, USA
[72] University of Rochester, Rochester, New York 14627, USA
[73] State University of New York, Stony Brook, New York 11794, USA
[74] Brookhaven National Laboratory, Upton, New York 11973, USA
[75] Langston University, Langston, Oklahoma 73050, USA
[76] University of Oklahoma, Norman, Oklahoma 73019, USA
[77] Oklahoma State University, Stillwater, Oklahoma 74078, USA
[78] Brown University, Providence, Rhode Island 02912, USA
[79] University of Texas, Arlington, Texas 76019, USA
[80] Southern Methodist University, Dallas, Texas 75275, USA
[81] Rice University, Houston, Texas 77005, USA
[82] University of Virginia, Charlottesville, Virginia 22901, USA and
[83] University of Washington, Seattle, Washington 98195, USA

(Dated: December 3, 2007)

We present a study of $\mu\mu\mu\mu$, $eeee$, and $\mu\mu ee$ events using 1 fb^{-1} of data collected with the D0 detector at the Fermilab Tevatron $p\bar{p}$ Collider at $\sqrt{s} = 1.96$ TeV. Requiring the lepton pair

masses to be greater than 30 GeV, we observe one event, consistent with the expected background of 0.13 ± 0.03 events and with the predicted standard model ZZ and $Z\gamma^*$ production of 1.71 ± 0.15 events. We set an upper limit on the ZZ and $Z\gamma^*$ cross section of 4.4 pb at the 95% C.L. We also derive limits on anomalous neutral trilinear ZZZ and $ZZ\gamma^*$ gauge couplings. The one-parameter 95% C.L. coupling limits with a form factor scale $\Lambda = 1.2$ TeV are $-0.28 < f_{40}^Z < 0.28$, $-0.31 < f_{50}^Z < 0.29$, $-0.26 < f_{40}^\gamma < 0.26$, and $-0.30 < f_{50}^\gamma < 0.28$.

PACS numbers: 12.15.Ji, 13.40.Em, 13.85.Qk

The standard model (SM) makes precise predictions for the couplings between gauge bosons based on the non-Abelian symmetries of the model. These predictions can be tested by studying di-boson production (WW, WZ, ZZ, $Z\gamma$, and $W\gamma$) at particle colliders. ZZ production is predicted to have the smallest cross section among the di-boson processes. Because the decay channels with the smallest expected background also have the smallest branching fractions, it has not been observed at a hadron collider. Nevertheless, the final states with small backgrounds may provide the best opportunity to observe the effects of physics beyond the SM. In addition to the production of new particles that could decay into ZZ, various extensions of the SM predict large anomalous values of the trilinear couplings [1] ZZZ and $ZZ\gamma^*$ that would result in higher cross sections than the SM prediction. The direct $ZZ\gamma^*$ and ZZZ couplings are zero in the SM. Consequently, an observation of an enhancement of the cross section would indicate physics beyond the SM.

Previous studies of ZZ production were made at the LEP electron-positron collider. The combined LEP results are available in Ref. [2]. All results are consistent with SM predictions. The CDF Collaboration searched for ZZ and WZ production in $p\bar{p}$ collisions at center-of-mass energy $\sqrt{s} = 1.96$ TeV with the result that $\sigma(ZZ) + \sigma(WZ) < 15.2$ pb at 95% C.L. [3] The predicted ZZ production cross section in the SM is 1.6 ± 0.1 pb at the Tevatron Collider energy [1, 4].

In this Letter, we present a search for ZZ and $Z\gamma^*$ production and a search for anomalous trilinear $ZZ\gamma^*$ and ZZZ couplings at the Fermilab Tevatron Collider with the D0 detector. We follow the framework of Ref. [1], where general ZZV ($V = Z$, γ) gauge and Lorentz-invariant interactions are considered. Such ZZV couplings can be parameterized by two CP-violating (f_4^V) and two CP-conserving (f_5^V) complex parameters. Additional anomalous couplings [5] can contribute when the Z bosons are off-shell. However, these couplings are highly suppressed near the Z boson resonance. We note that the ZZV couplings are distinct [1] from the $Z\gamma V$ couplings probed in $Z\gamma$ production in e^+e^- and hadronic collisions. Partial-wave unitarity is ensured by using a form-factor parameterization that causes the coupling to vanish at high parton center-of-mass energy $\sqrt{\hat{s}}$: $f_i^V = f_{i0}^V/(1+\hat{s}/\Lambda^2)^n$. Here, Λ is a form-factor scale, f_{i0}^V are the low-energy approximations of the couplings, and n is the form-factor power. In accordance with Ref. [1], we set $n = 3$ for all cases. The form-factor scale Λ is selected so that limits are within the values provided by unitarity at Tevatron Collider energies.

We search for ZZ and $Z\gamma^*$ production with a final state signature that consists of four leptons: two pairs of either electrons or muons. The electron and muon pairs can be produced either by the decay of an on-shell Z boson or via a virtual Z boson or photon. We studied three final states: four muon ($\mu\mu\mu\mu$), four electron ($eeee$), and two muons and two electrons ($\mu\mu ee$).

Data used in this analysis [6] were collected with the D0 detector at the Fermilab Tevatron $p\bar{p}$ collider at $\sqrt{s} = 1.96$ TeV between October 2002 and February 2006. The integrated luminosities [7] of the three channels are approximately 1 fb^{-1} each and are shown in Table I.

The D0 detector [8] is a multi-purpose detector designed to operate at high luminosity. The main components of the detector are an inner tracker, a liquid-argon/uranium calorimeter, and a muon system. The inner tracker consists of a silicon microstrip tracker (SMT) and a central fiber tracker (CFT) operating in a 2 Tesla solenoidal magnetic field. The SMT has coverage to pseudorapidity [9] $|\eta| \approx 3.0$, while the CFT has coverage to $|\eta| \approx 1.8$. The calorimeter system is outside the solenoid and has three cryostats, one for each of the two endcap calorimeters (EC) and one for the central calorimeter (CC). The CC covers the region $|\eta| < 1.1$, while endcap calorimeters extend the coverage to $|\eta| \approx 4$. The calorimeters are segmented along the shower direction with four layers forming the electromagnetic section (EM) and an additional three to five layers forming the hadronic section. This allows for electron-pion separation based on longitudinal and transverse shower shape. The muon system is outside of the calorimeters and consists of 1.8 Tesla iron toroid magnets with tracking chambers and scintillator counters mounted both inside and outside the toroid iron. The muon system extends to $|\eta| \approx 2$.

The D0 detector utilizes a three-level (L1, L2, and L3) trigger system. Electrons candidates are required to have deposited energy in the EM section of the calorimeter at L1 and L2, and then to satisfy selection criteria on shower shape and the fraction of energy in the EM calorimeter at L3. Muon candidates are required to have hits in the muon scintillation counters and a match with a track in the L1 track system. In a fraction of the data, muons are also required to have hits in the chambers of the muon

system. At L2, muon candidates are required to have track segments in the muon tracking detectors, and a minimum transverse momentum (p_T) is required. At L3, some muons are also required to have a match with a track from the inner tracker.

Combinations of single-electron and di-electron, as well as single-muon triggers are used in this analysis. These triggers have varying p_T and quality requirements on the leptons. The trigger efficiency for events with four high-p_T leptons that satisfy all other selection requirements is approximately 99%. In order to increase the collection efficiency, we do not require pairs of leptons to have opposite electric charge.

For the $\mu\mu\mu\mu$ channel, each muon is required to satisfy quality criteria based on scintillator and wire chamber information from the muon system and to have a matching track in the inner tracker. The track matched to the muon must have $p_T > 15$ GeV. Additionally, muons that are only identified in the muon detector layers before the toroid are required to have less than 2.5 GeV of total transverse energy deposited in the calorimeter in an annulus between $R = 0.1$ and $R = 0.4$ centered around the track matched to the muon [10]. Finally, the distance in the transverse plane of closest approach to the beamspot for the track matched to the muon must be less than 0.02 cm for tracks with SMT hits and less than 0.2 cm for tracks without SMT hits. This reduces the background from muons that do not originate from the primary vertex such as those from b decays and cosmic rays. The maximum distance between the muon track vertices for all muon pairs along the beam axis is required to be less than 3 cm. This reduces backgrounds from pairs of cosmic ray muons and from beam halo. Since the charge of the muons is not considered, three possible Z/γ^* combinations can be formed for each $\mu\mu\mu\mu$ event. Selected events are required to have the invariant masses of both muon pairs above 30 GeV for at least one of the combinations.

For the $eeee$ channel, each electron is required to have transverse energy (E_T) greater than 15 GeV, and to have $|\eta| < 1.1$ or $1.5 < |\eta| < 3.2$, and to be isolated from other energy clusters. Electrons are also required to satisfy identification criteria based on multivariate discriminators derived from calorimeter shower shape and tracking variables. Since the calorimeter fiducial region covers regions where there is little or no tracking coverage, only three of the four electrons are required to have an associated inner track. Electrons without a track match are required to satisfy more stringent shower shape requirements. Similar to the $\mu\mu\mu\mu$ channel, events are required to have the invariant masses of both electron pairs to be above 30 GeV for at least one of the three possible combinations.

For the $\mu\mu ee$ channel, muons are required to satisfy the same single muon selection criteria as in the $\mu\mu\mu\mu$ channel and electrons the same transverse energy and η criteria as in the $eeee$ channel. Both electrons are required to satisfy the multivariate discriminator based on shower shape and parameters of the matching inner track. In addition, electrons and muons are required to be separated by $R > 0.2$ to reduce backgrounds from muons that have radiated photons spatially coincident with a track. The invariant masses of the muon pair and the electron pair are required to be greater than 30 GeV.

We determine the total acceptance using a combination of information from MC and the data. We determine single electron and muon identification efficiencies directly from data [11], which contains high p_T electrons and muons from more than 100,000 single Z decays in each channel. Efficiencies are parameterized as functions of the relevant variables for the tracking, calorimeter and muon systems such as the position of the interaction along the beam direction and the η of the electron or muon. The acceptance for all channels is then determined using ZZ and $Z\gamma^*$ events generated with PYTHIA [12] and a parameterized simulation of the detector. The momenta of the muons and electrons are fluctuated in the Monte Carlo (MC) using angular and energy resolutions determined from the data, and the measured single electron and muon identification efficiencies are taken into account in calculating the acceptance. The number of observed events, the acceptance, and the expected signal calculated assuming the cross section is 1.6 pb are listed in Table I for each channel. Systematic uncertainties in acceptance due to momentum and energy scale calibrations, angular resolution, lepton identification variation with luminosity as well as other effects were included. Taking into account correlations between these uncertainties, a total of 1.71 ± 0.15 ZZ and $Z\gamma^*$ events is expected.

The main background sources are "Z + multi-jet" events, events where a top-antitop ($t\bar{t}$) quark pair is produced, and "combinatoric events", which are four-lepton events that survive because mis-paired leptons cause them to satisfy the dilepton invariant mass selection criteria when they would not have otherwise.

For a "Z + multi-jet" event to be a ZZ candidate, the jets are either mis-identified as electrons or muons or contain real electrons or muons from in-flight decays of pions, kaons, or heavy quarks. Though Z + jets (and γ^* + jets) events are the primary source of this background, it also includes those events where the Z boson or γ^* is reconstructed from one or more "fake" leptons. The "Z + multi-jet" event background is measured by first determining the probability for a jet in data to produce an electron or muon that satisfies the identification criteria. The probability for a jet to mimic a muon was measured in two-jet events selected via jet triggers. Muons that satisfy the selection criteria, have $p_T > 15$ GeV, and are found within $R < 0.2$ of the lower-E_T jet are considered "fake". The probability for a jet to mimic a muon is parameterized in terms of the tag-jet E_T. It is 10^{-4} for jets

Decay Channel	Luminosity (pb^{-1})	Acceptance	Expected Signal	Observed Events
$\mu\mu\mu\mu$	944 ± 58	0.27 ± 0.02	0.46 ± 0.05	0
eeee	1070 ± 65	0.23 ± 0.01	0.44 ± 0.03	0
$\mu\mu$ee	1020 ± 62	0.22 ± 0.02	0.81 ± 0.09	1

TABLE I: The integrated luminosity, acceptance (including lepton identification efficiencies), expected number of signal candidates, and the number of observed events in the three decay channels for the ZZ and $Z\gamma^*$ cross section analysis. A total of 1.71 ± 0.15 ZZ and $Z\gamma^*$ events is expected.

with $E_T \approx 15$ GeV and increases approximately linearly with E_T to 10^{-2} for jets with $E_T \approx 150$ GeV. The probability for a jet to mimic an electron was measured using a procedure similar to that described for muons. It is parameterized in terms of η and E_T to account for differences in the EC and CC and is typically 10^{-4} (10^{-2}) per jet for those electrons with (without) a track match. A systematic uncertainty of 30% is assigned to account for variations in the probabilities as a result of changes of the lepton identification criteria that were performed as cross checks. The probabilities for jets to be misidentified as muons are then applied to the jets in our $\mu\mu$ + jets data to determine the background to $\mu\mu\mu\mu$. Similarly appropriate probabilities are applied to $\ell\ell\ell$ + jet(s) events to determine the background to $eeee$ and $\mu\mu ee$. There, because we started from a three lepton sample, we correctly account for events with two real leptons, a photon misidentified as an electron, and a jet misidentified as either an electron or muon.

The background from $t\bar{t}$ events is determined from PYTHIA MC using a detailed GEANT-based [13] detector simulation program and the same reconstruction program that was used for the data.

The combinatoric background occurs only in the four-electron and four-muon decay channels. While it could be reduced by $\sim 1/3$ by requiring leptons which form Z bosons to have opposite signs, that would have resulted in a loss of signal efficiency for the high-p_T leptons that could result from anomalous couplings. This background was estimated using MC simulation. It is 0.016 ± 0.003 (0.015 ± 0.003) events in the $\mu\mu\mu\mu$ (eeee) channel; the uncertainty in the background comes from uncertainty in the lepton p_T resolution.

Table II displays the contributions of all non-negligible backgrounds and a summary for each decay channel. The total expected number of candidates from background sources is 0.13 ± 0.03 events.

One event is observed in data, consistent with the SM prediction of 1.71 ± 0.15 events plus background of 0.13 ± 0.03 events. We set an upper limit of 4.4 pb at the 95% C.L. on the cross section for $p\bar{p} \to ZZ + X$ and $Z\gamma^* + X$, where dilepton pair masses are greater than 30 GeV.

Because we do not observe an excess of events, we set limits on anomalous trilinear couplings by comparing the number of observed candidates with the predicted background and the expected sum of ZZ events from a MC program [1] using anomalous $ZZ\gamma^*$ and ZZZ couplings. We produced grids of MC samples by varying two of the anomalous couplings at a time. There are typically 5000 events generated at each grid point. These events are processed through the same detector and reconstruction simulation as was used in the cross section analysis. Because on-shell Z bosons dominate the contributions of the ZZV couplings in the MC and because off-shell Z bosons are enhanced by couplings [5] not implemented in the MC, we required the dilepton invariant mass to be > 50 (70) GeV for dimuons (dielectrons). This selection criterion is set by the resolution of the dilepton mass measurement and it removed the single $\mu\mu ee$ candidate event.

Background	$\mu\mu\mu\mu$	$eeee$	$\mu\mu ee$
Z + multi-jet	0.004 ± 0.001	0.065 ± 0.021	0.007 ± 0.002
$t\bar{t}$	0.010 ± 0.005	-	0.006 ± 0.003
Combinatoric	0.016 ± 0.003	0.015 ± 0.003	-
Beam Halo	0.003 ± 0.001	-	-
Total	0.033 ± 0.006	0.080 ± 0.021	0.013 ± 0.004

TABLE II: Contributions of non-negligible backgrounds to the expected number of candidates in the three decay channels for the cross section analysis. The total expected background is 0.13 ± 0.03 events.

The number of events expected for each choice of anomalous couplings was used to form a likelihood [6] for that point. Poisson probabilities were used for the expected signal plus background. These are convoluted with Gaussian uncertainties on the acceptance, background, and luminosity. One-dimensional (1D) and two-dimensional (2D) limits on anomalous couplings are formed by finding the coupling values with likelihood of 1.92 and 3.00 units greater than the minimum. Limits are determined using $\Lambda = 1.2$ TeV. The 95% C.L. 1D limits are $-0.28 < f_{40}^Z < 0.28$, $-0.26 < f_{40}^\gamma < 0.26$, $-0.31 < f_{50}^Z < 0.29$, and $-0.30 < f_{50}^\gamma < 0.28$. The 95% C.L. 2D contours f_{40}^γ vs. f_{40}^Z, f_{40}^γ vs. f_{50}^γ, f_{40}^Z vs. f_{50}^Z, and f_{50}^γ vs. f_{50}^Z are shown in Figure 1. In the four 2D cases the other two couplings are assumed to be zero.

In summary, we report results from a search for ZZ and $Z\gamma^*$ production using the $eeee$, $\mu\mu\mu\mu$ and $\mu\mu ee$ decay signatures. We analyzed 1 fb^{-1} of data collected with the D0 detector at the Fermilab Tevatron $p\bar{p}$ Collider at

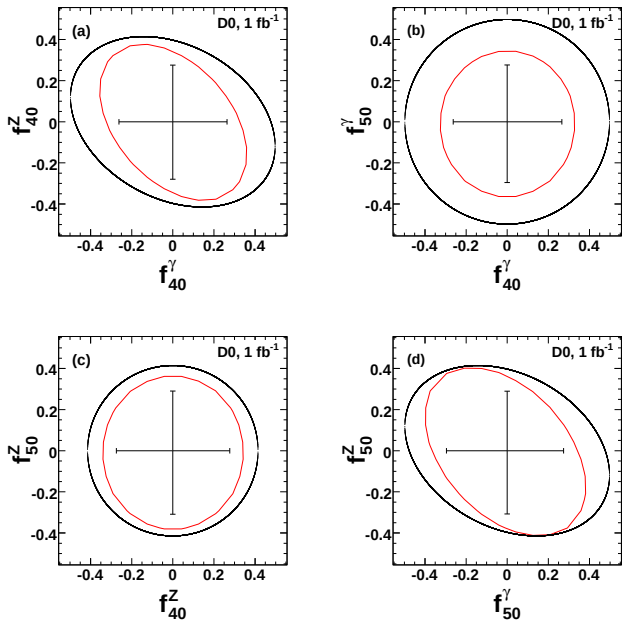

FIG. 1: Limits on anomalous couplings for $\Lambda = 1.2$ TeV: (a) f_{40}^{γ} vs. f_{40}^{Z}, (b) f_{40}^{γ} vs. f_{50}^{γ}, (c) f_{40}^{Z} vs. f_{50}^{Z}, and (d) f_{50}^{γ} vs. f_{50}^{Z}, assuming in each case that the other two couplings are zero. The inner and outer curves are the 95% C.L. two-degree of freedom exclusion contour and the constraint from the unitarity condition, respectively. The inner crosshairs are the 95% C.L. one-degree of freedom exclusion limits.

$\sqrt{s} = 1.96$ TeV. Requiring each lepton to have transverse momentum greater than 15 GeV, and the dilepton pair masses to be greater than 30 GeV, we observe one event with an expected SM background of 0.13 ± 0.03 events. The one observed event is consistent both with background and with predicted SM ZZ and $Z\gamma^*$ production of 1.71 ± 0.15 events. We set an upper limit of 4.4 pb at the 95% C.L. on the cross section for $p\bar{p} \to ZZ + X$ and $Z\gamma^* + X$, where dilepton pair masses are greater than 30 GeV. This is the most restrictive cross section limit for ZZ production at the Tevatron. We set limits on anomalous neutral trilinear ZZZ and $ZZ\gamma^*$ gauge couplings. These represent the first bounds on these anomalous couplings from the Tevatron. Limits on f_{40}^{Z}, f_{50}^{Z}, and f_{50}^{γ} are more restrictive than those of the combined LEP experiments [2].

We thank the staffs at Fermilab and collaborating institutions, and acknowledge support from the DOE and NSF (USA); CEA and CNRS/IN2P3 (France); FASI, Rosatom and RFBR (Russia); CAPES, CNPq, FAPERJ, FAPESP and FUNDUNESP (Brazil); DAE and DST (India); Colciencias (Colombia); CONACyT (Mexico); KRF and KOSEF (Korea); CONICET and UBACyT (Argentina); FOM (The Netherlands); Science and Technology Facilities Council (United Kingdom); MSMT and GACR (Czech Republic); CRC Program, CFI, NSERC and WestGrid Project (Canada); BMBF and DFG (Germany); SFI (Ireland); The Swedish Research Council (Sweden); CAS and CNSF (China); Alexander von Humboldt Foundation; and the Marie Curie Program.

[a] Visitor from Augustana College, Sioux Falls, SD, USA.
[b] Visitor from The University of Liverpool, Liverpool, UK.
[c] Visitor from ICN-UNAM, Mexico City, Mexico.
[d] Visitor from II. Physikalisches Institut, Georg-August-University Göttingen, Germany.
[e] Visitor from Helsinki Institute of Physics, Helsinki, Finland.
[f] Visitor from Universität Zürich, Zürich, Switzerland.
[†] Fermilab International Fellow.
[‡] Deceased.

[1] U. Baur and D. Rainwater, Phys. Rev. D **62**, 113011 (2000).
[2] The LEP Collaborations: ALEPH, DELPHI, L3, and OPAL, "A Combination of Preliminary Electroweak Measurements and Constraints on the Standard Model", arXiv:hep-ex/0612034.
[3] CDF Collaboration, D. Acosta *et al.*, Phys. Rev. D **71**, 091105(R) (2005).
[4] J. M. Campbell and R. K. Ellis, Phys. Rev. D **60**, 072002 (1999).
[5] G. J. Gounaris, J. Layssac, and F. M. Renard, Phys. Rev. D **62**, 073012 (2000).
[6] C. Jarvis, Ph. D thesis, University of Maryland, 2007 (unpublished).
[7] T. Andeen *et al.*, FERMILAB-TM-2365 (2007).
[8] DØ Collaboration, V. Abazov *et al.*, Nucl. Instrum. Methods A **565**, 463 (2006).
[9] The D0 coordinate system is cylindrical with the z-axis along the proton beamline and the polar and azimuthal angles denoted as θ and ϕ respectively. The pseudorapidity is defined as $\eta = -\ln\tan(\theta/2)$.
[10] The variable R between two objects i and j is defined as $R = \sqrt{(\eta_i - \eta_j)^2 + (\phi_i - \phi_j)^2}$.
[11] DØ Collaboration, V. Abazov *et al.*, Phys. Rev. D **76**, 052006 (2007).
[12] T. Sjöstrand *et al.*, Comp. Phys. Commun. **135**, 238 (2001).
[13] R. Brun and F. Carminati, CERN Program Library Long Writeup W5013, 1993 (unpublished).